

# Multi-Channel Attentive Feature Fusion for Radio Frequency Fingerprinting

Yuan Zeng, Yi Gong, Jiawei Liu, Shangao Lin, Zidong Han, Ruoxiao Cao, Kaibin Huang and Khaled Ben Letaief

**Abstract**—Radio frequency fingerprinting (RFF) is a promising device authentication technique for securing the Internet of things. It exploits the intrinsic and unique hardware impairments of the transmitters for RF device identification. In real-world communication systems, hardware impairments across transmitters are subtle, which are difficult to model explicitly. Recently, due to the superior performance of deep learning (DL)-based classification models on real-world datasets, DL networks have been explored for RFF. Most existing DL-based RFF models use a single representation of radio signals as the input. Multi-channel input model can leverage information from different representations of radio signals and improve the identification accuracy of the RF fingerprint. In this work, we propose a novel multi-channel attentive feature fusion (McAFF) method for RFF. It utilizes multi-channel neural features extracted from multiple representations of radio signals, including IQ samples, carrier frequency offset, fast Fourier transform coefficients and short-time Fourier transform coefficients, for better RF fingerprint identification. The features extracted from different channels are fused adaptively using a shared attention module, where the weights of neural features from multiple channels are learned during training the Mcaff model. In addition, we design a signal identification module using a convolution-based ResNeXt block to map the fused features to device identities. To evaluate the identification performance of the proposed method, we construct a WiFi dataset, named WFDI, using commercial WiFi end-devices as the transmitters and a Universal Software Radio Peripheral (USRP) as the receiver. Experimental results on WFDI show that the proposed Mcaff model outperforms single-channel-based RFF models in terms of identification accuracy and robustness. Moreover, comparative experiments between the proposed framework and a baseline RFF model without attention-based feature fusion show that the proposed shared attention module has the advantage of improving the identification accuracy of RF fingerprint.

**Index Terms**—Radio frequency fingerprinting, feature fusion, convolutional neural network, attention mechanism

## I. INTRODUCTION

With the help of recent technology advances in wireless electronic devices and beyond fifth-generation (B5G) communication systems, Internet of Things (IoT) technology has

been further developed and plays an increasingly important role in our daily life, such as facilitating human-to-machine communication or machine-to-machine communication. The evolution of IoT tends to enable ubiquitous connectivity, where billions of tiny embedded wireless devices, enabling sensing, computing, and communications, are deployed everywhere. Wireless security is a critical challenge for IoT applications, since mobile devices in a wireless communication network are vulnerable to malicious attacks when operating in an open environment. Impersonation attacks are one of the most common and threatening malicious attacks in wireless communication networks. Device authentication that validates whether the devices or users are legitimate enables to protect the wireless devices from impersonation attacks and improves the security of IoT. Traditional authentication methods were designed by employing software addresses, such as Internet Protocol (IP) or Media Access Control (MAC), as identity and using classical cryptography-based authentication techniques [1]. Cryptography algorithms usually rely on complicated mathematical operations or protocols [2]. However, due to limitations in power consumption and computation resources, such complex cryptography algorithms may be undesirable in many IoT applications such as smart cities [3] and intelligent industries [4]. An efficient alternative tool for wireless security is radio frequency fingerprinting (RFF), which uses waveform-level imperfections imposed by the RF circuit to obtain a fingerprint of the wireless device. The imperfections normally include in-phase and quadrature (IQ) imbalance, phase offset, frequency offset, sampling offset, and phase noise [5], which are unique and can hardly be imitated by adversarial devices.

RFF is a standard pattern recognition problem and usually consists of two stages: learning and inference. During the learning phase, signals are gathered from end-devices and processed to learn a classification model at a server. After that, the server will use the trained model to authenticate end-devices during the inference phase. Compared with conventional cryptography-based security schemes, RFF, by operating at the physical layer, does not impose any additional computational burden and power consumption on end-devices. On the other hand, the receiver/server is usually equipped with sufficient computational resources and energy, which is capable of gathering signals from multiple end devices and doing signal learning and inference. Such arrangement of computational resources and capabilities among the receiver/server and end-devices is particularly desirable for many IoT applications, since most end-devices are low-cost with limited computational and energy resources.

Traditional RFF methods are proposed based on carefully

Y. Zeng is with the Academy for Advanced Interdisciplinary Studies, Southern University of Science and Technology (SUSTech), Shenzhen, 518055, P. R. China. (e-mail: zengy3@sustech.edu.cn).

Y. Gong, S. Lin and Z. Han are with the Department of Electrical and Electronic Engineering, SUSTech, Shenzhen, P. R. China. (e-mail: gongy@sustech.edu.cn, linsa2019@mail.sustech.edu.cn, hanzd@sustech.edu.cn).

J. Liu and K. Huang are with the Department of Electrical and Electronic Engineering, The University of Hong Kong, Hong Kong. (e-mail: liujw@eee.hku.hk, huangkb@eee.hku.hk).

R. Cao and K. B. Letaief are with the Department of Electronic and Computer Engineering, The Hong Kong University of Science and Technology, Hong Kong. (e-mail: rcaoah@connect.ust.hk, eekhaled@ust.hk).

hand-crafting specialized feature extractors and classifiers. Manually extracting handcrafted features requires prior comprehensive knowledge of the communication system, such as channel state and communication protocol. In addition, it is difficult to extract features of hardware imperfection accurately, since the hardware imperfections are interrelated. By performing feature extraction and signal classification at two separate stages, traditional RFF methods may work well when the extracted features are distinguishable for classifiers. However, the identification performance of classifiers is highly dependent on the quality of extracted features, and an efficient feature extraction method for one scenario may easily fail in another.

Recently, deep learning (DL)-based RFF methods have been proposed to fingerprint radios through learning of the hardware impairments [6], [7], since DL-based methods automatically optimize feature extraction by minimizing the identification error. Different neural network architectures, such as convolutional neural networks (CNNs) [8], recurrent neural networks (RNNs) [9] and long short-term memory (LSTM) [10], have been explored for automatic RFF and shown better RF device identification performance than traditional RFF methods. Early DL-based methods mainly use the received IQ samples as the input of a DL network [11]–[13]. More recently, a few DL-based RFF methods tend to explore the specific characteristics of radio signals, such as bispectrum [12], Hilbert spectrum [13] and differential constellation trace figure [14], for RFF. Utilizing multiple signal representations as the input data of an RFF model may further improve the performance of RFF models, since different signal representations can provide different views of the radio signals. In [15], a hybrid classification framework was proposed to weight multiple features of radio signals with pre-calculated weights for RFF. However, obtaining an efficient fusion of different representations is a complex task and pre-calculated weights may produce sub-optimal identification results in practical applications. We thus face the problem of designing an effective learning method to learn multi-channel fusion of different signal representations in an end-to-end manner for better RF device identification.

In general, training and test data are collected at different times and locations. However, hardware impairments may change across days due to temperature or voltage oscillations, there may be only limited samples for learning, and wireless channel may become unstable due to time-varying fading and noise. Although a lot of progress has been made in RFF on radio signals with high signal-to-noise ratio (SNR) conditions, the identification performance still drops sharply when the end-devices are deployed in the presence of electromagnetic interference, environment noises, or other low SNR conditions. A few recent DL-based methods [7], [16] proposed model-based augmentation strategies to improve the robustness of the DL-based RFF models, and validated the proposed strategies using simulated RF devices and nonlinear effects. These methods provided possible solutions to improve identification accuracy when practical RF devices and nonlinear characteristics are similar to the simulations. It is still a challenging task to improve the robustness of RFF methods in noisy environments.

To tackle the above issues, this work proposes a multi-

channel attentive feature fusion (McAFF) method to adaptively fuse multi-channel neural features for RFF. The network fuses neural features extracted from multi-channel inputs including IQ samples, carrier frequency offset (CFO), fast Fourier transform (FFT) coefficients, and short-time Fourier transform (STFT) coefficients in an end-to-end learning manner. In addition, a shared attention module is designed to learn weights regarding feature importance for RFF. The entire model is trained in a supervision manner using WiFi data.

To evaluate the proposed McAFF model, we design an RF signal acquisition system, by using a Universal Software Radio Peripheral (USRP) software defined radio (SDR) platform as the receiver and 72 commercial WiFi end-devices as the target devices. We collect WiFi signal transmitted using the standard IEEE 802.11n protocol over several experiment days, and use the legacy-short training field (L-STF) sequence in the collected uplink frames to construct a dataset for RFF, named WFDI. Extensive experiments are conducted to evaluate the identification performance of the proposed McAFF model. Experimental results demonstrate the effectiveness of the proposed McAFF model on WiFi device identification. The main contributions of our work are summarized as follows.

- A novel McAFF model that exploits the complementary information from different representations of radio signals is introduced for RF fingerprint identification. It addresses RFF by optimizing the combination of multi-channel features and utilizes a convolution layer to attend to important features for better identification performance of RF fingerprint.
- We design a signal identification module using a convolution-based ResNeXt block to map the fused neural features to device identities for automatic RFF.
- We design a WiFi signal acquisition system that collects WiFi signal of 72 commercial WiFi end-devices and construct a new experimental dataset WFDI aimed at evaluating the identification performance of DL-based RFF methods.
- We provide an extensive ablation study of different signal representations and analyze the rationality of the proposed attention module through comparative experiments. Experimental results demonstrate that the proposed McAFF model outperforms baseline models that use a specific signal representation as input in terms of identification accuracy. In addition, we analyze the impact of different data scales and collection dates on the identification performance. Experimental results show that the proposed McAFF model is more robust against to noisy radio signals, and changes in data scale and collection time.

The rest of the paper is organized as follows. Related work is given in Section II. The problem statement is given in Section III. In Section IV, we give details about how we generate our Dataset. Then in Section V, we briefly introduce the signal pre-processing and representation algorithms. Later, we describe the proposed McAFF model-based RFF method in detail in Section VI. The performance of the proposed method is illustrated and analyzed with experiments in Section VII.

Finally, conclusions are drawn in Section VIII.

## II. RELATED WORK

### A. RF Fingerprinting

A variety of approaches have been proposed for RFF. Early RFF methods typically perform feature extraction and classification separately. Existing hand-tailored feature extraction techniques can be roughly divided into three categories: transient-based (TB) techniques, spectrum-based (SB) techniques, and modulation-based (MB) techniques. TB methods extract the signal variations in the turn-on/off transient, such as the transient signal envelope [17] and phase offset [18]. These methods use time domain signal processing algorithms to extract features from received signals. SB methods extract frequency domain features, such as power spectrum density (PSD) [19], [20], Hilbert spectrum [13], and time-frequency statistics [21]. MB features including IQ offset [22], clock skew [23], [24], CFO [25], [26], sampling frequency offset [27], etc, can be extracted from the received baseband signal. During the classification process, the authenticator will first feed the extracted features to train the classifier and then infer the device identity. Typical classification algorithms include support vector machine (SVM) [22] and K-nearest neighbor (KNN) [28]. The identification performance of these classifiers relies heavily on feature extraction, and hand-tailored feature extraction techniques require comprehensive knowledge of communication technology and protocol, which limits the practical applications.

In the past few years, DL, which uses a cascade of multiple layers of nonlinear processing units for feature extraction and transformation, has achieved great success in image classification and speech recognition. Recently, it has also been studied to solve physical-layer communication problems including channel estimation [29], [30], modulation recognition [31]–[33] and RFF [34]–[36]. Compared to traditional RFF methods, DL-based RFF methods use DNNs to automatically extract more distinguishable and high-level features by learning a mapping strategy from training data. A CNN-based RFF model, operating on the error signal obtained after subtracting out an estimated ideal signal from frequency-corrected data, was proposed in [8]. Riyaz et al. [7] evaluated the effectiveness of an optimized CNN architecture on RFF and introduced artificial impairments to improve the identification accuracy. Cekic et al. [16] investigated the identification performance of a complex-valued DNN on WiFi and ADS-B signals. Sankhe et al. [6] used a 16-node USRP SDR testbed and an external database of more than 100 WiFi devices to generate a WiFi dataset and introduced a robust CNN architecture for device identification using raw IQ samples. In [37], an impairment hopping spread spectrum method that identifies a radio through a random pseudo-noise binary sequence was proposed. Shen et al. [35] evaluated the impact of different signal representations including spectrogram, IQ samples, and FFT coefficients on a CNN-based RFF model, and designed a hybrid classifier using the softmax output and CFO to improve the RF fingerprint identification performance of the CNN-based RFF scheme on LoRa devices. Shawabka et al.

[11] investigated the identification performance of CNN-based RFF models on a large-scale dataset with 10,000 WiFi and ADS-B devices. In contrast, this work proposes to improve RF fingerprint identification performance using multi-channel attention fusion and CNN.

### B. Multi-channel Signal Classification

Our work is more closely related to multi-channel signal classification, where multiple signal representations are used to provide classifiers with richer information from different views. Peng et al. [15] proposed to combine four modulation features including differential constellation trace figure, CFO, modulation offset, and IQ offset with the weights pre-calculated according to the estimated SNR and evaluated the effectiveness of the proposed feature fusion method on RFF using a KNN classifier. In [38] a multi-channel learning framework was proposed to exploit the complementary information from IQ multi-channel, I channel, and Q channel data for automatic modulation recognition. Lin et al. [39] introduced a dual-channel spectrum fusion module to include an original signal channel and a filtered signal channel for modulation recognition. Inspired by existing multi-channel-based classifiers, we use four signal representations, namely IQ samples, CFO, FFT coefficients, and STFT coefficients, as the input of our RFF model. However, in contrast to combining the four signal features using manually designed weights, our study tackles the problem of adaptively weight features extracted from the four signal representations for RFF.

### C. Attention-based Fusion

Recently, attention mechanism [40] allows the network to automatically find target related features and enhance the related features while diminishing other features, and it has achieved state-of-the-art performance on various natural language processing and computer vision tasks [41]–[43]. Fan et al. [44] proposed a deep attention-based fusion algorithm to dynamically control the weights of the spatial and spectral features and combine them deeply. Xu et al. [45] presented a co-attention mechanism to guide the fusion of RGB and infrared multi-spectral information for semantic segmentation. For wireless communication, attention mechanisms have been investigated in DL-based modulation classification models to improve classification performance. O'Shea et al. [46] designed an attention mechanism to learn a localization network for blindly synchronizing and normalizing radio signals. Lin et al. [47] proposed a time-frequency attention mechanism to learn which channel, time, and frequency information are more important for modulation recognition. In this work, we design a shared attention module to adaptively fuse neural features extracted from multi-channel inputs.

## III. PROBLEM STATEMENT

In wireless communication systems, the received signal is generally down-converted to baseband, filtered, and sampled, and the complex baseband samples are processed to extract the information bits. The baseband samples are not only

degraded by non-ideal channel and noise but also related to non-idealities of RF and analog parts, including sampling clock offset, power amplifier, phase noise, and CFO. In this section, we first briefly introduce the origin and representation of several classic RF hardware impairments, including IQ imbalance, CFO, and power amplifier (PA) nonlinearity, in the form of mathematical models. Later, we introduce the task of RFF.

### A. Mathematical Model of RF Impairments

Let  $x_b(t)$  denote the transmitted baseband complex signal at time  $t$ ,  $x_{b,I}(t)$  and  $x_{b,Q}(t)$  denote the in-phase (I) and quadrature (Q) information of the baseband signal  $x_b(t)$ , respectively. The complex baseband signal  $x_b(t)$  can be expressed as

$$x_b(t) = x_{b,I}(t) + jx_{b,Q}(t) = r(t)e^{j\phi(t)}, \quad (1)$$

where  $j = \sqrt{-1}$  denotes the imaginary unit,  $r(t)$  and  $\phi(t)$  denote the amplitude and phase of  $s(t)$ , respectively. The ideal RF signal emitted from a wireless transmitter can be modeled as

$$x(t) = x_{b,I}(t)\cos(2\pi f_c t) + x_{b,Q}(t)\sin(2\pi f_c t), \quad (2)$$

where  $x(t)$  is the transmitted RF signal without hardware impairment, and  $f_c$  is the carrier frequency. However, the transmitted RF signal generated by practical transmitters will be distorted due to the inevitable hardware imperfections in the transmitters' analog RF chain, as shown in Fig. 1. IQ imbalance, CFO, and nonlinear distortions of the power amplifier are three typical RF impairments in actual hardware implementations, they can be modeled as follows:

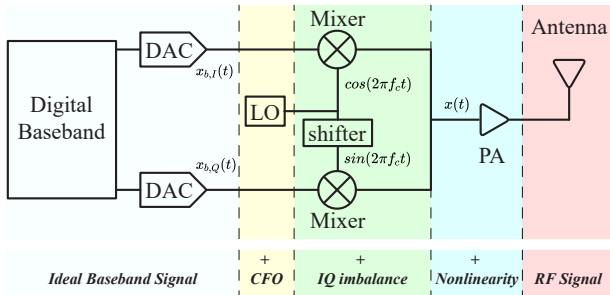


Fig. 1: The origins of signal distortions in the transmitter.

**IQ imbalance:** In the RF chain of a transmitter, the in-phase (I) and quadrature (Q) baseband signals are up-converted to the cosine and sine carrier waves using two independent quadrature mixers. The cosine and sine carrier waves are generated by the local oscillator (LO) of the transmitter. The ideal sine carrier wave is a copy of the cosine carrier wave delayed by  $\pi/2$ . However, quadrature mixers are often impaired by gain and phase mismatches between the parallel sections of the RF chain dealing with the I and Q signal paths. The gain mismatch causes amplitude imbalance, and phase deviation from  $\pi/2$  results in phase imbalance. Assume that the gain error is  $20 \log [g_1/g_2]$  dB and the phase error is  $\varepsilon_p$  degrees. Then the IQ imbalance can be modeled as:

$$g_1 \cos(2\pi f_{c,t} - \varepsilon_p/2), \text{ and } g_2 \sin(2\pi f_{c,t} + \varepsilon_p/2), \quad (3)$$

where  $f_{c,t}$  is the center frequency that depends on the LO of the transmitter.

**Non-linear Distortions of Power Amplifier:** The power amplifiers are usually used in the RF chain to amplify the pass-band signal for transmission. In practice, the analog amplification process in PA will incur nonlinear distortions in both amplitude and phase. These effects are directly applied to the pass-band signal but can be equivalently modeled on baseband signals. An empirical baseband model of PA was presented in [48]. Let  $g(t)$  and  $\phi(t)$  denote the amplitude and phase offset of the PA output, respectively. They can be modeled as

$$g(t) = \frac{\alpha_a r(t)}{1 + \beta_a [r(t)]^2}, \quad (4)$$

and

$$\phi(t) = \frac{\alpha_\phi r(t)^2}{1 + \beta_\phi [r(t)]^2}, \quad (5)$$

where  $\alpha_a, \alpha_\phi, \beta_a$  and  $\beta_\phi$  are fitting parameters extracted from measurement results. The equivalent baseband signal of PA output, denoted by  $\tilde{x}_b(t)$ , is then given by

$$\tilde{x}_b(t) = g(t)e^{j[\phi(t) + \varepsilon_\phi(t)]}. \quad (6)$$

**Carrier Frequency Offset:** The transmitted signals are collected by an RF receiver in a practical end-to-end communication system. The carrier frequencies used for up-conversion and down-conversion are generated in the transmitter and receiver using their own LOs, respectively, which can never oscillating at an identical frequency. Let  $y(t)$  denote the ideal signal received at a receiving antenna, the received signal  $y(t)$  is down-converted to the baseband by a mixer, which is given by

$$y_b(t) = y(t)e^{-j\omega_r t}, \quad (7)$$

where  $y_b(t)$  is the received baseband signal at time  $t$ , and  $\omega_r = 2\pi f_{c,r}$  denotes the angular frequency with continuous-time signals of the receiver with  $f_{c,r}$  local carrier frequency of the receiver. Let  $\varepsilon_f$  denote the carrier frequency offset between the transmitter and receiver (e.g.,  $f_{c,r} = f_{c,t} + \varepsilon_f$ ). The received baseband signal  $y_b(t)$  can be expressed using  $f_{c,t}$  as

$$y_b(t) = y(t)e^{-j2\pi(f_{c,t} + \varepsilon_f)t}, \quad (8)$$

and the carrier waves generated by the receiver's LO can then be modeled as

$$\cos(2\pi(f_{c,t} + \varepsilon_f)t), \text{ and } \sin(2\pi(f_{c,t} + \varepsilon_f)t). \quad (9)$$

### B. Radio Frequency Fingerprinting

RFF refers to the task of identifying radio devices, which is typically done by analyzing their transmitted RF signals and extracting RF fingerprints associated with their hardware impairments. An RFF system is illustrated in Fig. 2, which consists of a receiver and massively deployed wireless devices. This work considers RFF as an independent third party in a wireless communication system to differentiate the identities of wireless devices using their uplink RF signals. Specifically, the user devices first transmit data to the access point using a predefined communication protocol. Then, their uplink signals

are captured by a receiver equipped on the edge server. This work aims at identifying practical RF devices using the received baseband signals at the receiver. Given the received baseband signal  $y_b(t)$ , the server performs a series of signal processing and classification algorithms on  $y_b(t)$  to identify the RF devices.

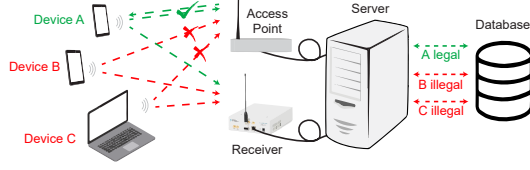


Fig. 2: Illustration of RFF system.

#### IV. DATASET

To evaluate the RF fingerprint identification performance of RFF algorithms, we design an RF signal acquisition system, as illustrated in Fig. 3. The system consists of a wireless access point (AP) for establishing links with end-devices using WiFi, WiFi end-devices for transmitting WiFi signals to the AP, a National Instrument (NI) USRP-2922 SDR platform for gathering the WiFi signals from end-devices, and a server for processing the received signals collected at the SDR. The RF signal acquisition system is placed in a  $3\text{m} \times 3\text{m} \times 3\text{m}$  anechoic chamber testbed. The chamber can absorb unwanted radio frequency waves by lining the chamber with hundreds of blue foam protruding arrowheads. Using this isolated environment can help to reduce the wireless channel impact and accent the device fingerprint. This is because the transmission inside the chamber is not affected by external RF activity, and the cones deployed in the chamber absorb signals generated internally, preventing multi-path effect.

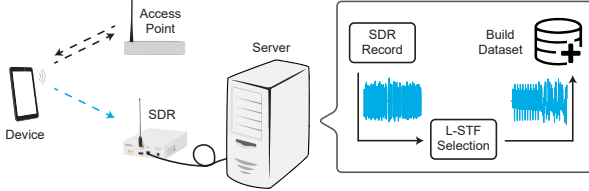


Fig. 3: The radio frequency signal acquisition system.

We collect baseband IQ samples transmitted using the standard IEEE 802.11n WiFi protocol [49], which is one of the most common wireless communication protocols used nowadays. The signal from WiFi end-devices is streamed at 2.472GHz (channel 13) with 20MHz bandwidth. The IQ data sampled by the SDR is then saved for the RFF.

##### A. WFDI Dataset

We use 72 commercial WiFi end-devices as the target devices. During the data collection, all devices are configured to transmit WiFi signals in legacy or mixed mode, resulting in a preamble-payload structure with the same legacy-short training field (L-STF) in the collected uplink frames, as shown in Fig. 4. SDR receives the transmitted signal, operating

at center frequency of 2.472GHz and baseband sampling rate of 20MSa/s. Each WiFi device sends the uplink frames repeatedly during the transmission. Each uplink frame consists of randomly generated data samples and the same L-STF sequence, as shown in Fig. 5. For each device, one-second (1s) data is captured by SDR and saved in the sever per recording day. The data collection process is repeated for 8 days.

Frame detection is a standard process to detect signal arrival and locate uplink frames in the IEEE 802.11 WiFi communication protocol. The packet preamble consists of a 20us signal, where the first 16us signal is primarily used for synchronization. In our experiments, we use a short training field (STF) for frame detection, which is performed on the recorded one-second data to locate the initial sample of each uplink frame. We randomly select  $N_m = 256$  L-STF sequences with  $N_s = 160$  samples each from the one-second IQ data for each device and construct our WiFi Device Identification (WFDI) dataset using all L-STF sequences recorded in  $N_d = 8$  experiment days. The L-STF signals are saved as a matrix, with the dimension of  $N_n \times N_d \times N_m \times N_c \times N_s$ .  $N_n = 72$  is the number of target WiFi devices and  $N_c = 2$  represents I and Q channels.

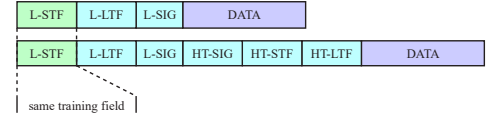


Fig. 4: The WiFi package in legacy and mixed transmission mode. The legacy mode consists of L-STF, legacy-long training field (L-LTF), legacy-signal field (L-SIG) and data, and the mixed mode consists of L-STF, L-LTF, L-SIG, high throughput-signal field (HT-SIG), high throughput-short training field (HT-STF), high throughput-long training field (HT-LTF) and data.

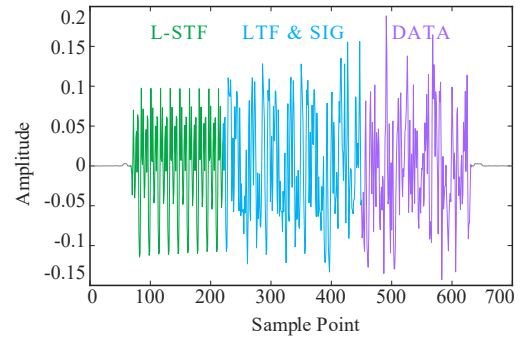


Fig. 5: An example of an uplink frame.

#### V. SIGNAL PREPROCESSING AND REPRESENTATION

A discrete-time version of the baseband signal  $y_b(t)$  in Eq. (8), denoted by  $y(n)$ , can be obtained by sampling from the continuous-time signal using an analog-to-digital converter (ADC) at uniformly spaced times  $T_s$ , associated with a sampling rate  $f_s = \frac{1}{T_s}$ . The data model of  $y(n)$  is then given by

$$y(n) = y_b(t)|_{t=nT_s}, -\infty < n < \infty, \quad (10)$$

In this work, we first perform energy normalization to remove energy differences between RF devices, then we adopt CFO estimation, FFT coefficients, and STFT coefficients to represent the non-idealities of RF.

#### A. Energy Normalization:

The energy of the WiFi signal is one of the standard features used in signal classification, which is susceptible to transmission distance. Since RFF aims at identifying devices by learning hardware imperfections imposed by the RF circuit, rather than energy differences, we perform energy normalization to bring the average amplitude to a target level using the root-mean-square of the amplitude of the signal  $y(n)$ . The normalized version of  $y(n)$  is given by

$$y_e(n) = \frac{y(n)}{\sqrt{\frac{1}{N} \sum_{n=0}^{N-1} y^2(n)}}. \quad (11)$$

where  $N$  is the signal length and  $y_e(n)$  denotes the normalized signal at time sampling index  $n$ . The L-STF sequences of the signal  $y_e(n)$ , denoted by  $\tilde{y}(n)$ , are then used to extract characteristics of the RF fingerprint.

#### B. Signal Representation

**CFO Estimation:** CFO is caused by the difference between the LO of the transmitter and receiver, and results in the phase offset of the received baseband IQ samples, see Eq. (8). The CFO can be estimated with the help of the received preambles. This work adopts a coarse estimation algorithm in [50] to estimate CFO, that is,

$$\hat{\epsilon}_f = \frac{1}{16} \angle \left( \sum_{n=0}^{N_s-17} \tilde{y}^*(n) \tilde{y}(n+16) \right) \quad (12)$$

where  $\angle(\cdot) \in [-\pi, \pi]$  is the angle of a complex variable, and  $(\cdot)^*$  denotes conjugation. The phase difference between  $\tilde{y}(n)$  and  $\tilde{y}(n+16)$  indicates the accumulated CFO over 16 samples. Then, we conduct a vector using the phase information of the CFO estimation to represent the signal  $\tilde{y}(n)$ , that is,

$$\mathbf{R}_{CFO} = [\angle(\tilde{y}^*(0)\tilde{y}(16)), \dots, \angle(\tilde{y}^*(N_s-17)\tilde{y}(N_s-1))]^T. \quad (13)$$

**FFT Coefficients:** Given the signal  $\tilde{y}(n)$ , a fast Fourier transform (FFT) is performed to compute the discrete Fourier transform (DFT) of the sequence and transform the complex symbols into the frequency domain, i.e.,

$$Y_{FFT}(f) = \sum_{n=0}^{N_s-1} \tilde{y}(n) e^{-j2\pi f n / N_s}, f = 0, \dots, N_s - 1, \quad (14)$$

where  $Y_{FFT}(f)$  is the FFT coefficients at frequency-bin index  $f$ . We then use the FFT coefficients, defined by  $\mathbf{R}_{FFT} = [Y_{FFT}(0), \dots, Y_{FFT}(N_s-1)]^T$ , as a frequency-domain representation of the signal  $\tilde{y}(n)$ .

**STFT Coefficients:** Short-time Fourier transform (STFT) is a sequence of DFTs of a windowed signal. Unlike FFT where DFT provides the averaged frequency information over the entire signal, STFT computes the time-localized frequency information for situations where frequency components of a

signal vary over time [51]. Let  $w(\cdot)$  denote a window function of length  $J$  and let  $K$  be the window shift. The signal  $\tilde{y}(n)$  is windowed and transformed into the frequency domain by applying a DFT, i.e.,

$$Y_{STFT}(m, f) = \sum_{n=mK}^{mK+J-1} \tilde{y}(n) w(n-mK) e^{-j\omega_f(n-mK)}, \quad (15)$$

where  $Y_{STFT}(m, f)$  denotes the STFT coefficients at discrete-time frame index  $m$  and frequency-bin index  $f$ , and  $\omega_f = 2\pi f / J$  is the discrete frequency variable at frequency-bin index  $f$ . We use the STFT coefficients  $Y_{STFT}(m, f)$ ,  $\forall m, \forall f$  as another representation of the signal  $\tilde{y}(n)$ , denoted as  $\mathbf{R}_{STFT}$ .

## VI. LEARNING FEATURE FUSION FOR RF FINGERPRINTING

This section introduces the proposed McAFF model for RFF. The model consists of two functional parts: multi-channel feature fusion and signal identification. Instead of simply stacking multi-channel inputs including IQ samples, CFO, FFT coefficients and STFT coefficients, a deep attention fusion algorithm is utilized to combine them deeply, which uses a shared attention module (SAM) to adaptively fuse multi-channel neural features. Later, a ResNeXt block [52] based signal identification module (SIM) is performed for device identification. Given multi-channel inputs, denoted as  $\mathbf{R} = \{\mathbf{R}_{IQ}; \mathbf{R}_{CFO}; \mathbf{R}_{FFT}; \mathbf{R}_{STFT}\}$ , the model  $\mathcal{F}_{\mathbf{w}}$  is trained to minimize the cross-entropy loss function, that is,

$$\hat{\mathbf{w}} = \operatorname{argmin}_{\mathbf{w}} \mathbb{E}_{\mathbf{R}, \tilde{y}} (\mathcal{L}(\mathcal{F}_{\mathbf{w}}(\mathbf{R}), \tilde{y})), \quad (16)$$

where  $\mathbb{E}(\cdot)$  denotes the expectation operation and  $\mathcal{L}(\mathcal{F}_{\mathbf{w}}(\mathbf{R}), \tilde{y})$  is the cross-entropy loss between the estimation result  $\mathcal{F}_{\mathbf{w}}(\mathbf{R})$  and the true label  $\tilde{y}$ . Fig. 6 illustrates an overview of the proposed McAFF model, we describe the details of each part as follows.

#### A. Multi-channel Feature Fusion

The multi-channel feature fusion part first uses four channel features  $\mathbf{R}$  as input data. Then the four streams of input data are fed to four separate convolutional layers to acquire four channel neural features, denoted by  $\mathbf{F}_{IQ}$ ,  $\mathbf{F}_{CFO}$ ,  $\mathbf{F}_{FFT}$  and  $\mathbf{F}_{STFT}$ , respectively. Specifically, the settings of the convolutional layers used to process  $\mathbf{R}_{CFO}$  and  $\mathbf{R}_{FFT}$  are the same, i.e., one dimensional (1D) convolutional layer with 128 channels and filter size of  $1 \times 7$ . A 1D convolutional layer with 128 channels and filter size of  $2 \times 7$  is performed to extract neural features of  $\mathbf{R}_{IQ}$ , and a 2D convolutional layer with 128 channels and filter size of  $8 \times 7$  is used to process  $\mathbf{R}_{STFT}$ . Then, SAM is adopted to refine the intermediate neural features  $\mathbf{F}_{IQ}$ ,  $\mathbf{F}_{CFO}$ ,  $\mathbf{F}_{FFT}$  and  $\mathbf{F}_{STFT}$ .

Given a feature map  $\mathbf{F} \in \mathbb{R}^{C \times H \times W}$  with  $C$  the number of feature map channels and  $H \times W$  the size of feature maps, SAM aims at inferring a 2D shared attention map  $\mathbf{M} \in \mathbb{R}^{3 \times H \times W}$  to adaptively control the weight of each point on input feature map. The refined feature map  $\mathbf{F}_r \in \mathbb{R}^{C \times H \times W}$  is given by

$$\mathbf{F}_r = \mathbf{M}(\mathbf{F}) \otimes \mathbf{F}, \quad (17)$$



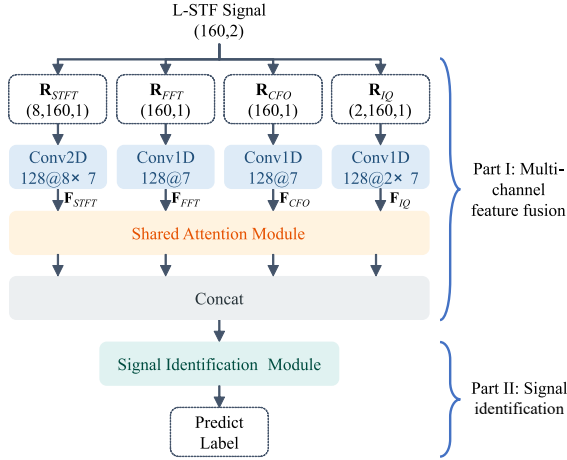


Fig. 6: Overview of the proposed McAFF model. Given an input L-STF signals, part I extracts multi-channel neural features from multi-channel signal representations of the input signals, and adaptively fuse the multi-channel neural features using a shared attention module. Then the fused features will go through the signal identification part to obtain device identity.

where  $\otimes$  is element-wise multiplication. During multiplication, the important parts of input feature map are enhanced, and the rest ones are faded out according to the learned attention weights  $\mathbf{M}$ .

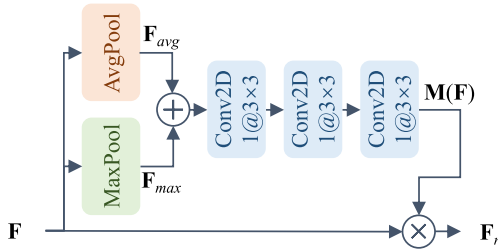


Fig. 7: Structure of the proposed shared attention module.

As illustrated in Fig. 7, SAM first aggregates spatial information by performing average-pooling and max-pooling on the input feature map  $\mathbf{F}$  in parallel, generating two different spatial context features, denoted by  $\mathbf{F}_{avg} \in \mathbb{R}^{H \times W}$  and  $\mathbf{F}_{max} \in \mathbb{R}^{H \times W}$ , respectively. The two context features are then concatenated and convolved by three 2D convolutional layers to infer the attention map  $\mathbf{M}$ . The attention map can be expressed as:

$$\mathbf{M}(\mathbf{F}) = \sigma(v_3^{3 \times 3}([\mathbf{F}_{avg}; \mathbf{F}_{max}]]), \quad (18)$$

where  $\sigma$  is the Sigmoid function, and  $v_3^{3 \times 3}$  denotes three cascaded convolutional layers. Then, neural feature map on each channel is refined as in Eq. (17). After that, the four-channel refined neural features are concatenated to generate the fused features  $\mathbf{F}_{r,c} \in \mathbb{R}^{4C \times H \times W}$ , which is given by

$$\mathbf{F}_{r,c} = [\mathbf{F}_{r,IQ}; \mathbf{F}_{r,CFO}; \mathbf{F}_{r,FFT}; \mathbf{F}_{r,STFT}] \quad (19)$$

The fused features  $\mathbf{F}_{r,c}$  are then fed to the signal identification for fingerprinting.

### B. Signal Identification

The signal identification part includes SIM, which maps refined features to device identities. As illustrated in Fig. 8, SIM consists of a convolution-based ResNeXt block [52], two fully connected (FC) layers and a softmax layer. ResNeXt block is designed to build a simple and highly modularized network architecture for image classification. It aggregates a set of transformations with the same topology and exploits the split-transform-merge strategy in an easy and extensible way. Compared with ResNet [53], ResNeXt block-based neural network is able to improve classification accuracy by increasing the size of the set of transformations. Let  $\mathbf{x} = [x_1, \dots, x_D]$  denote a  $D$ -channel input vector to a neuron and  $w_i$  denote the weight of a filter for the  $i$ th channel. A simple neuron in deep neural networks performs the inner product of the input vector and its corresponding weights, which can be thought of a form of aggregating transformation:

$$\sum_{i=1}^D w_i x_i. \quad (20)$$

Such inner product operation is the elementary transformation in fully-connected and convolutional layers. Inspired by the inner production operation, ResNeXt presents a more generic operation by replacing the elementary transformation  $w_i x_i$  with an arbitrary function  $\Gamma_i(\mathbf{x})$ , that is,

$$\sum_{i=1}^C \Gamma_i(\mathbf{x}), \quad (21)$$

where  $C$  is the size of the set of transformations to be aggregated. As shown in Fig. 8, the ResNeXt block processes the input feature map  $\mathbf{F}_{r,c}$  by using the residual function with the aggregated transformations in Eq. (21). The ResNeXt block generates an output  $\mathbf{F}_b$  from an input  $\mathbf{F}_r$  through the following:

$$\mathbf{F}_b = \mathbf{F}_{r,c} + \sum_{i=1}^C \Gamma_i(\mathbf{F}_{r,c}). \quad (22)$$

The ResNeXt block consists of three convolution-based operations: a single 2D convolutional layer with 128 channels and filter size of  $1 \times 1$ , a grouped convolutional layer performs  $C = 32$  groups of convolutions with 128 channels and filter size of  $3 \times 3$ , and a single 2D convolutional layer with 256 channels and filter size of  $1 \times 1$ . The ResNeXt block is followed by two fully-connected layers with 512 neurons each and finally an output layer with the softmax function. In addition, each convolutional and fully-connected layer is followed by batch normalization [54] and Rectified Linear Unit (ReLU) [55].

## VII. EXPERIMENTS

### A. Experimental setup

We use five experiments to evaluate and analyze the identification performance of the proposed McAFF model. First,

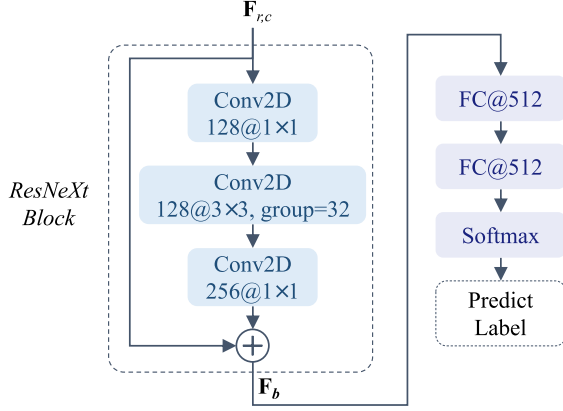


Fig. 8: Illustration of the proposed signal identification module.

we study the effect of the different signal representation approaches including IQ samples, CFO, FFT, STFT, and a combination of the four on identification accuracy and feature modeling efficiency. We denote the identification models using single signal representation IQ samples, CFO, FFT, and STFT as MIQ, MCFO, MFFT, and MSTFT, respectively. Second, we consider that training and test data are collected on the same day. We select all signals collected on one day from the dataset and split the signals into training and test data. We evaluate the identification performance of the proposed McAFF model on different days. Later, we evaluate our model using training and test data collected from different days, i.e., samples collected from one or several days are used for training, and data collected from the remaining days are used for test. After that, we analyze the effectiveness of the deep attention fusion algorithm on RFF. Finally, we evaluate the identification performance of the proposed McAFF model in a simulated noisy environment, where white Gaussian noise is deliberately introduced to modify the original data and increase the size and variability of the initial dataset WFDI.

### B. Implementation details

We convert the L-STF signals to frequency domain using frame-based STFT, with a frame length  $J = 120$  and a 95%-overlapping Hamming window. For each device, WFDI consists of  $N_t = N_d \times N_m$  IQ signals. To evaluate the identification performance of RFF methods on a training dataset of different sizes, we randomly select a certain percentage of data from the  $N_t$  signals. All experiments are implemented using Keras with Tensorflow backbone and trained on a PC with an NVIDIA TITAN X GPU. The identification model is trained with a batch size of 256 and optimized with Adam optimizer [56]. The learning rate starts with 0.001 and decays 0.1 when the validation loss does not drop within 10 epochs. The training is terminated when the validation loss does not drop within 15 epochs, and the model with the smallest validation loss is saved and used for test.

### C. Experimental results

**Ablation study of different signal representations:** We do ablation studies to illustrate the impact of signal representations on RF device identification accuracy. The training curves

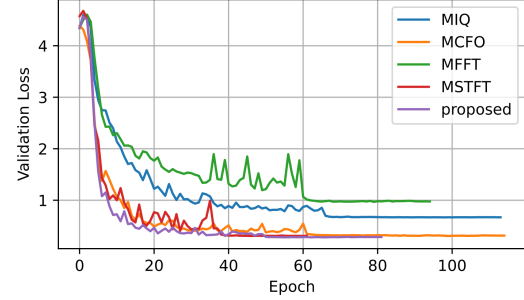


Fig. 9: Validation loss of RFF models versus training epochs on WFDI with data size of  $2\%N_t$ . Compared with single-channel RFF models, including MIQ, MCFO, MFFT and MSTFT, the proposed McAFF model converges faster and to a lower validation loss.

TABLE I: RFF performance comparison between MIQ, MCFO, MFFT, MSTFT and the proposed McAFF.

	$1\%N_t$	$5\%N_t$	$15\%N_t$	$25\%N_t$	$50\%N_t$
MIQ	64.52%	91.17%	95.95%	97.21%	98.29%
MCFO	86.69%	96.06%	97.92%	98.38%	98.94%
MFFT	47.37%	86.43%	93.27%	94.3%	96.17%
MSTFT	89.94%	95.18%	96.81%	97.41%	98.01%
McAFF	<b>90.00%</b>	<b>96.11%</b>	<b>97.94%</b>	<b>98.41%</b>	<b>99.01%</b>

of all models are shown in Fig. 9. We evaluate model efficiency in terms of identification accuracy versus training data size. Table I shows the experimental results. When the training data size is larger than  $50\%N_t$ , all models get enough accuracy (higher than 96%) for device identification. The identification performance of the proposed model is better than those of all other models on training datasets of different sizes. Compared with MIQ, MCFO, MFFT, and MSTFT, the proposed model gets higher identification accuracy and is more robust for training data scales. In addition, MSTFT performs better than MIQ, MCFO, and MFFT when the training data size is small, such as  $1\%N_t$ . This can be explained that STFT with time-frequency information provides a richer representation of signal than IQ samples, CFO and FFT.

**“Train and test same day” scenario:** We first split our WFDI dataset according to the collection date and name a sub-dataset collected on the day  $i$  as  $DAY_i$ . After that, each sub-dataset is partitioned as follows: 70% for training, 10% for validation, and 20% for test. We train an identification model on each sub-dataset and get 8 models in total. Table II shows the identification results of the proposed method on different sub-datasets. We observe that the proposed McAFF model works well when training and test data are collected on the same day. Specifically, the proposed McAFF model



TABLE II: RF identification performance of the proposed McAFF in the “Train and Test Same Day” scenario.

	$DAY_1$	$DAY_2$	$DAY_3$	$DAY_4$	$DAY_5$	$DAY_6$	$DAY_7$	$DAY_8$
McAFF	99.17%	98.25%	99.26%	99.62%	99.01%	99.6%	98.21%	<b>99.87%</b>

TABLE III: RF identification performance comparison between MIQ, MCFO, MFFT, MSTFT and the proposed McAFF model in the “Train and test different day” scenario.

	1_train/7_test	2_train/6_test	3_train/5_test	4_train/4_test
MIQ	58.78%	75.81%	79.76%	82.81%
MCFO	62.44%	75.26%	78.9%	81.18%
MFFT	70.22%	81.39%	84.58%	86.45%
MSTFT	<b>76.10%</b>	85.43%	86.52%	88.06%
McAFF	75.35%	<b>86.04%</b>	<b>87.72%</b>	<b>88.67%</b>

TABLE IV: Effect of Attentive Fusion in the “Train and test different day” scenario.

	1_train/7_test	2_train/6_test	3_train/5_test	4_train/4_test
McAFF (no attentive fusion)	73.96%	85.26%	86.6%	88.06%
McAFF	<b>75.35%</b>	<b>86.04%</b>	<b>87.72%</b>	<b>88.67%</b>

achieves the highest identification rate of 99.85% on  $DAY_8$ , and the minimum recognition rate is 98.21% on  $DAY_7$ . The average identification accuracy of the proposed McAFF model over eight days is 99.12%.

**“Train and test different day” scenario:** In this experiment, we consider a scenario that training and test data are collected on different days. Table III shows the experimental results. We observe that the identification accuracy of MIQ, MCFO and MFFT decreases dramatically when training and test data are collected from different dates. MSTFT gets around 2% to 6% higher identification accuracy than MIQ, MCFO and MFFT. When data collected from one day is used for training and data collected from remaining 7 days is used for test (1\_train/7\_test), the proposed method gets 0.8% lower identification accuracy than MSTFT, and around 5%, 13% and 17% higher identification accuracy than MFFT, MCFO and MIQ, receptively. By using samples collected from multiple days for training, all RFF models gets significant performance gains, i.e., around 10% higher identification accuracy. Specifically, the proposed method gets around 0.7% higher identification accuracy than MSTFT, and around 3% to 11% higher identification accuracy than MCFO, MFFT and MIQ. This can be explained that the proposed method uses multi-channel inputs and adaptively fuses the multi-channel neural features is more robustness to data collection dates.

**Effect of SAM:** We compare the proposed McAFF model with a baseline model which simply concatenates multi-channel features without attention module. Table IV shows identification performance comparison results. Compared with the baseline model, the proposed McAFF model gets better identification performance on training datasets of different data sizes. This is because that the proposed McAFF model utilizes attention fusion to dynamically control the weights of multi-channel neural features.

**Impact of noise:** This subsection studies the effect of different levels of noise on the identification accuracy of the

proposed method and single-channel RFF models. Table V lists the identification accuracy of the proposed method and all single-channel RFF models at 6 different SNR levels. It shows that the identification accuracy of all RFF models is increased with increasing the SNR level of the input data, and increased with increasing the amount of training samples. In addition, the proposed method significantly outperforms single-channel RFF models. For single-channel RFF models, all models gets similar identification accuracy when  $1\%N_t$  data is used for training. MSTFT and MIQ gets similar identification accuracy at all SNR levels, and around 2% to 10% higher identification accuracy than MFFT. The identification accuracy of the MFFT is around 2% to 10% higher than those of the MCFO. Fig. 10 illustrates the RF fingerprint identification performance comparison results in a scenario where training and test data are collected from different days. Compared with single-channel RFF models, the proposed method gets better identification performance at all SNR levels. The experiment results demonstrate that the proposed method using multi-channel attention fusion neural network is more effective for RFF when the received radio signals are noisy.

## VIII. CONCLUSION

In this work, we proposed a novel multi-channel attentive feature fusion (McAFF) model for RFF. The proposed model consists of two sequential parts: multi-channel feature fusion for feature learning and fusion, and signal identification for RF device identification. The multi-channel feature fusion part first computes the representations of the input WiFi signals using the CFO estimation, FFT and STFT. Then, a shared attention module was used to adaptively control the weight of the neural features learned from the four channel inputs, including IQ samples, CFO, FFT coefficients and STFT coefficients. The model was trained to minimize the cross-entropy loss function for WiFi device identification. To evaluate the effectiveness of the proposed McAFF model on RF fingerprint

TABLE V: RFF performance comparison between MIQ, MCFO, MFFT, MSTFT and the proposed McAFF at different SNR levels.

	2 dB		4 dB		6 dB		8 dB		10 dB		12 dB	
	1% $N_t$	50% $N_t$	1% $N_t$	50% $N_t$	1% $N_t$	50% $N_t$	1% $N_t$	50% $N_t$	1% $N_t$	50% $N_t$	1% $N_t$	50% $N_t$
MIQ	8.44%	39.46%	11.12%	46.97%	13.61%	48.54%	17.48%	57.01%	22.06%	66.65%	27.02%	74.68%
MCFO	8.84%	18.33%	11.43%	23.28%	14.36%	30.08%	18.5%	37.79%	23.94%	46.18%	30.28%	54.18%
MFFT	10.12%	30.53%	12.78%	36.51%	15.67%	43.41%	19.77%	50.12%	20.9%	57.8%	23.7%	64.44%
MSTFT	9.19%	37.81%	11.43%	44.08%	14.37%	51.78%	17.6%	60.38%	21.32%	67.58%	24.22%	72.57%
McAFF	<b>15.02%</b>	<b>42.46%</b>	<b>18.98%</b>	<b>49.95%</b>	<b>22.71%</b>	<b>59.14%</b>	<b>26.83%</b>	<b>65.95%</b>	<b>31.65%</b>	<b>73.45%</b>	<b>35.87%</b>	<b>79.16%</b>

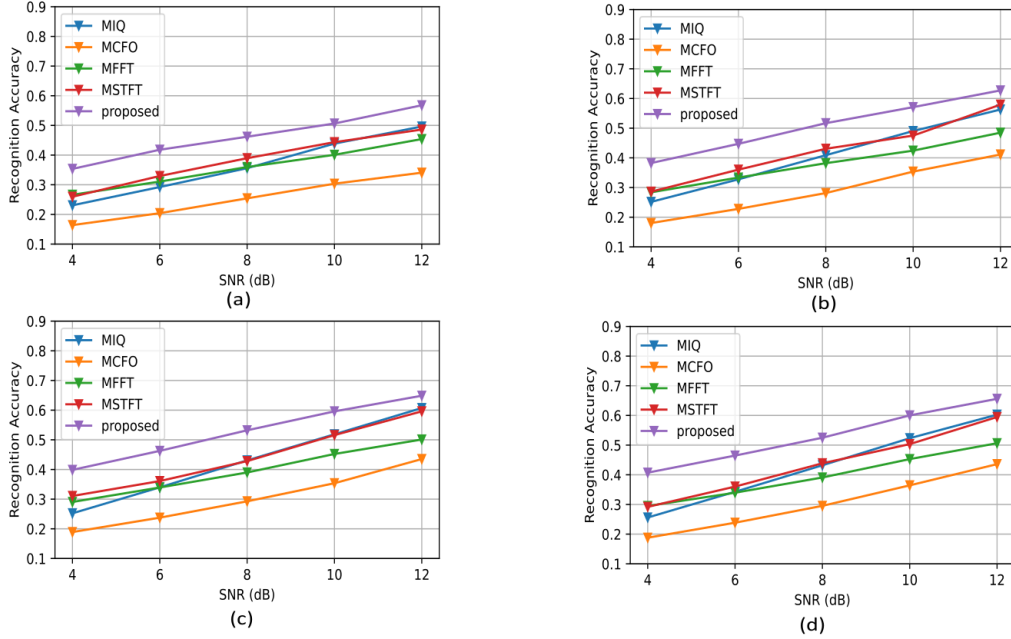


Fig. 10: RF fingerprint identification accuracy of the proposed method, MIQ, MCFO, MFFT and MSTFT versus SNR in the “Train and test different day” scenario. (a) 1 train\_7 test; (b) 2 train\_6 test; (c) 3 train\_5 test; (d) 4 train\_4 test.

identification from real-world RF signals, we designed a new dataset (WFDI), including 2GB wireless data captured from 72 WiFi end-devices over the course of 8 days in an anechoic chamber. We provided an exhaustive evaluation of the impact of signal representation on RF fingerprint identification performance, and analyzed the effectiveness of the proposed shared attention module in terms of fingerprinting accuracy in a scenario where training and test data are collected from different days. In addition, we evaluated the identification effect of the proposed McAFF model on a simulated noisy dataset. Experimental results demonstrated that the proposed RFF model with multi-channel attentive feature fusion gets better RF fingerprint identification accuracy on datasets of different sizes and collection dates, and is more robust against to noisy radio signals.

Learning to fuse multi-channel features is a straightforward idea to improve the designing of a feature-based RF fingerprinting system. This work conducts an extensive research on how to compose multi-channel features and signal identification for better RFF, which has been demonstrated in a real RF signal acquisition system. However, similar to other supervised signal classification methods, the proposed McAFF model does not address dynamic wireless communi-

cation systems with wireless channel and environmental noise variations. How to leverage blind signal processing algorithms or learning-based signal enhancement models to help extract robust features of RF impairments at the test stage is an interesting direction for future work.

## IX. ACKNOWLEDGMENTS

This work is supported in part by National Natural Science Foundation in China under Grants 62071212 and 62106095, Guangdong Basic and Applied Basic Research Foundation under Grant 2019B1515130003, Shenzhen Science and Technology Program under Grants JCYJ202001091414409 and KCXFZ20211020174802004.

## REFERENCES

- [1] Y. Zou, J. Zhu, X. Wang, and L. Hanzo, “A survey on wireless security: Technical challenges, recent advances, and future trends,” *Proceedings of the IEEE*, vol. 104, no. 9, pp. 1727–1765, 2016.
- [2] D. He and S. Zeadally, “An analysis of RFID authentication schemes for internet of things in healthcare environment using elliptic curve cryptography,” *IEEE Internet of Things Journal*, vol. 2, no. 1, pp. 72–83, 2014.
- [3] A. Zanella, N. Bui, A. Castellani, L. Vangelista, and M. Zorzi, “Internet of things for smart cities,” *IEEE Internet of Things Journal*, vol. 1, no. 1, pp. 22–32, 2014.

- [4] N. Lu, N. Cheng, N. Zhang, X. Shen, and J. W. Mark, "Connected vehicles: Solutions and challenges," *IEEE Internet of Things Journal*, vol. 1, no. 4, pp. 289–299, 2014.
- [5] E. O. Johnson, "Physical limitations on frequency and power parameters of transistors," in *Semiconductor Devices: Pioneering Papers*, 1991, pp. 295–302.
- [6] K. Sankhe, M. Belgiovine, F. Zhou, S. Riyaz, S. Ioannidis, and K. Chowdhury, "ORACLE: optimized radio classification through convolutional neural networks," in *Proceedings of IEEE Computer Communications (INFOCOM)*, Paris, France, 2019, pp. 370–378.
- [7] S. Riyaz, K. Sankhe, S. Ioannidis, and K. Chowdhury, "Deep learning convolutional neural networks for radio identification," *IEEE Communications Magazine*, vol. 56, no. 9, pp. 146–152, 2018.
- [8] K. Merchant, S. Revay, G. Stantchev, and B. Nossain, "Deep learning for RF device fingerprinting in cognitive communication networks," *IEEE Journal of Selected Topics in Signal Processing*, vol. 12, no. 1, pp. 160–167, 2018.
- [9] S. Rajendran, W. Meert, D. Giustiniano, V. Lenders, and S. Pollin, "Deep learning models for wireless signal classification with distributed low-cost spectrum sensors," *IEEE Transactions on Cognitive Communications and Networking*, vol. 4, no. 3, pp. 433–445, 2018.
- [10] R. Das, A. Gadre, S. Zhang, S. Kumar, and J. M. Moura, "A deep learning approach to IoT authentication," in *Proceedings of IEEE International Conference on Communications (ICC)*, 2018, pp. 1–6.
- [11] A. Al-Shawabka, F. Restuccia, S. D'Oro, T. Jian, B. C. Rendon, N. Soltani, J. Dy, S. Ioannidis, K. Chowdhury, and T. Melodia, "Exposing the fingerprint: Dissociating the impact of the wireless channel on radio fingerprinting," in *Proceedings of IEEE Computer Communications (INFOCOM)*, 2020, pp. 646–655.
- [12] J. Gong, X. Xu, and Y. Lei, "Unsupervised specific emitter identification method using radio-frequency fingerprint embedded InfoGAN," *IEEE Transactions on Information Forensics and Security*, vol. 15, pp. 2898–2913, 2020.
- [13] Y. Pan, S. Yang, H. Peng, T. Li, and W. Wang, "Specific emitter identification based on deep residual networks," *IEEE Access*, vol. 7, pp. 54 425–54 434, 2019.
- [14] L. Peng, J. Zhang, M. Liu, and A. Hu, "Deep learning based RF fingerprint identification using differential constellation trace figure," *IEEE Transactions on Vehicular Technology*, vol. 69, no. 1, pp. 1091–1095, 2019.
- [15] L. Peng, A. Hu, J. Zhang, Y. Jiang, J. Yu, and Y. Yan, "Design of a hybrid RF fingerprint extraction and device classification scheme," *IEEE Internet of Things Journal*, vol. 6, no. 1, pp. 349–360, 2018.
- [16] M. Cekic, S. Gopalakrishnan, and U. Madhow, "Robust wireless fingerprinting: Generalizing across space and time," *arXiv preprint arXiv:2002.10791*, 2020.
- [17] H. J. Patel, M. A. Temple, and R. O. Baldwin, "Improving ZigBee device network authentication using ensemble decision tree classifiers with radio frequency distinct native attribute fingerprinting," *IEEE Transactions on Reliability*, vol. 64, no. 1, pp. 221–233, 2014.
- [18] D. A. Knox and T. Kunz, "Practical RF fingerprints for wireless sensor network authentication," in *Proceedings of the 8th International Wireless Communications and Mobile Computing Conference (IWCMC)*, 2012, pp. 531–536.
- [19] W. C. Suski II, M. A. Temple, M. J. Mendenhall, and R. F. Mills, "Using spectral fingerprints to improve wireless network security," in *Proceedings of IEEE Global Telecommunications Conference (GLOBECOM)*, 2008, pp. 1–5.
- [20] A. C. Polak and D. L. Goeckel, "Identification of wireless devices of users who actively fake their rf fingerprints with artificial data distortion," *IEEE Transactions on Wireless Communications*, vol. 14, no. 11, pp. 5889–5899, 2015.
- [21] T. J. Bihl, K. W. Bauer, and M. A. Temple, "Feature selection for RF fingerprinting with multiple discriminant analysis and using ZigBee device emissions," *IEEE Transactions on Information Forensics and Security*, vol. 11, no. 8, pp. 1862–1874, 2016.
- [22] V. Brik, S. Banerjee, M. Gruteser, and S. Oh, "Wireless device identification with radiometric signatures," in *Proceedings of the 14th ACM international conference on Mobile computing and networking*, 2008, pp. 116–127.
- [23] T. Kohno, A. Broido, and K. C. Claffy, "Remote physical device fingerprinting," *IEEE Transactions on Dependable and Secure Computing*, vol. 2, no. 2, pp. 93–108, 2005.
- [24] S. Jana and S. K. Kasera, "On fast and accurate detection of unauthorized wireless access points using clock skews," *IEEE Transactions on Mobile Computing*, vol. 9, no. 3, pp. 449–462, 2009.
- [25] M. Leonardi, L. Di Gregorio, and D. Di Fausto, "Air traffic security: Aircraft classification using ADS-B message's phase-pattern," *Aerospace*, vol. 4, no. 4, p. 51, 2017.
- [26] J. Hua, H. Sun, Z. Shen, Z. Qian, and S. Zhong, "Accurate and efficient wireless device fingerprinting using channel state information," in *Proceedings of IEEE Computer Communications (INFOCOM)*, 2018, pp. 1700–1708.
- [27] T. D. Vo-Huu, T. D. Vo-Huu, and G. Noubir, "Fingerprinting Wi-Fi devices using software defined radios," in *Proceedings of the 9th ACM Conference on Security & Privacy in Wireless and Mobile Networks*, 2016, pp. 3–14.
- [28] I. O. Kennedy, P. Scanlon, F. J. Mullany, M. M. Buddhikot, K. E. Nolan, and T. W. Rondeau, "Radio transmitter fingerprinting: A steady state frequency domain approach," in *Proceedings of IEEE 68th Vehicular Technology Conference*, 2008, pp. 1–5.
- [29] R. Lippmann, "An introduction to computing with neural nets," *IEEE Assp Magazine*, vol. 4, no. 2, pp. 4–22, 1987.
- [30] H. He, C.-K. Wen, S. Jin, and G. Y. Li, "Model-driven deep learning for mimo detection," *IEEE Transactions on Signal Processing*, vol. 68, pp. 1702–1715, 2020.
- [31] T. J. O'Shea, J. Corgan, and T. C. Clancy, "Convolutional radio modulation recognition networks," in *Proceedings of the International Conference on Engineering Applications of Neural Networks*, 2016, pp. 213–226.
- [32] Y. Zeng, M. Zhang, F. Han, Y. Gong, and J. Zhang, "Spectrum analysis and convolutional neural network for automatic modulation recognition," *IEEE Wireless Communications Letters*, vol. 8, no. 3, pp. 929–932, 2019.
- [33] Y. Wang, G. Gui, T. Ohtsuki, and F. Adachi, "Multi-task learning for generalized automatic modulation classification under non-gaussian noise with varying snr conditions," *IEEE Transactions on Wireless Communications*, vol. 20, no. 6, pp. 3587–3596, 2021.
- [34] N. Soltanieh, Y. Norouzi, Y. Yang, and N. C. Karmakar, "A review of radio frequency fingerprinting techniques," *IEEE Journal of Radio Frequency Identification*, vol. 4, no. 3, pp. 222–233, 2020.
- [35] G. Shen, J. Zhang, A. Marshall, L. Peng, and X. Wang, "Radio frequency fingerprint identification for LoRa using spectrogram and CNN," in *Proceedings of IEEE Computer Communications (INFOCOM)*, 2021, pp. 1–10.
- [36] Y. Li, Y. Ding, J. Zhang, G. Goussetis, and S. K. Podilchak, "Radio frequency fingerprinting exploiting non-linear memory effect," *IEEE Transactions on Cognitive Communications and Networking*, pp. 1–1, 2022.
- [37] K. Sankhe, M. Belgiovine, F. Zhou, L. Angioloni, F. Restuccia, S. D'Oro, T. Melodia, S. Ioannidis, and K. Chowdhury, "No radio left behind: Radio fingerprinting through deep learning of physical-layer hardware impairments," *IEEE Transactions on Cognitive Communications and Networking*, vol. 6, no. 1, pp. 165–178, 2019.
- [38] J. Xu, C. Luo, G. Parr, and Y. Luo, "A spatiotemporal multi-channel learning framework for automatic modulation recognition," *IEEE Wireless Communications Letters*, vol. 9, no. 10, pp. 1629–1632, 2020.
- [39] S. Lin, Y. Zeng, and Y. Gong, "Modulation recognition using signal enhancement and multistage attention mechanism," *IEEE Transactions on Wireless Communications*, vol. 21, no. 11, pp. 9921–9935, 2022.
- [40] A. Vaswani, N. Shazeer, N. Parmar, J. Uszkoreit, L. Jones, A. N. Gomez, L. Kaiser, and I. Polosukhin, "Attention is all you need," *Advances in Neural Information Processing Systems*, vol. 30, 2017.
- [41] N. Moritz, T. Hori, and J. Le Roux, "Semi-supervised speech recognition via graph-based temporal classification," in *Proceedings of IEEE International Conference on Acoustics, Speech and Signal Processing (ICASSP)*, 2021, pp. 6548–6552.
- [42] Y. Zhao and D. Wang, "Noisy-reverberant speech enhancement using denseunet with time-frequency attention," in *Proceedings of the 21st Annual Conference of the International Speech Communication Association*, 2020, pp. 3261–3265.
- [43] S. Woo, J. Park, J.-Y. Lee, and I. S. Kweon, "CBAM: convolutional block attention module," in *Proceedings of the European Conference on Computer Vision (ECCV)*, 2018, pp. 3–19.
- [44] C. Fan, B. Liu, J. Tao, J. Yi, and Z. Wen, "Spatial and spectral deep attention fusion for multi-channel speech separation using deep embedding features," *arXiv preprint arXiv:2002.01626*, 2020.
- [45] J. Xu, K. Lu, and H. Wang, "Attention fusion network for multi-spectral semantic segmentation," *Pattern Recognition Letters*, vol. 146, pp. 179–184, 2021.
- [46] T. J. O'Shea, L. Pemula, D. Batra, and T. C. Clancy, "Radio transformer networks: Attention models for learning to synchronize in wireless systems," in *Proceedings of the 50th Asilomar Conference on Signals, Systems and Computers*, 2016, pp. 662–666.

- [47] S. Lin, Y. Zeng, and Y. Gong, "Learning of time-frequency attention mechanism for automatic modulation recognition," *IEEE Wireless Communications Letters*, vol. 11, no. 4, pp. 707–711, 2022.
- [48] J. C. Pedro and S. A. Maas, "A comparative overview of microwave and wireless power-amplifier behavioral modeling approaches," *IEEE Transactions on Microwave Theory and Techniques*, vol. 53, no. 4, pp. 1150–1163, 2005.
- [49] "IEEE standard for information technology–telecommunications and information exchange between systems - local and metropolitan area networks–specific requirements - part 11: Wireless lan medium access control (MAC) and physical layer (PHY) specifications," *IEEE Std 802.11-2020 (Revision of IEEE Std 802.11-2016)*, pp. 1–4379, 2021.
- [50] E. Sourour, H. El-Ghorrury, and D. McNeill, "Frequency offset estimation and correction in the IEEE 802.11 a WLAN," in *Proceedings of IEEE 60th Vehicular Technology Conference, 2004. VTC2004-Fall. 2004*, vol. 7, 2004, pp. 4923–4927.
- [51] N. Kehtarnavaz, "CHAPTER 7 - frequency domain processing," in *Digital Signal Processing System Design (Second Edition)*. Burlington: Academic Press, 2008, pp. 175–196.
- [52] S. Xie, R. Girshick, P. Dollár, Z. Tu, and K. He, "Aggregated residual transformations for deep neural networks," in *Proceedings of IEEE Conference on Computer Vision and Pattern Recognition (CVPR)*, 2017, pp. 1492–1500.
- [53] K. He, X. Zhang, S. Ren, and J. Sun, "Deep residual learning for image recognition," in *Proceedings of IEEE Conference on Computer Vision and Pattern Recognition (CVPR)*, 2016, pp. 770–778.
- [54] S. Ioffe and C. Szegedy, "Batch normalization: Accelerating deep network training by reducing internal covariate shift," in *Proceedings of the International Conference on Machine Learning (ICML)*, F. R. Bach and D. M. Blei, Eds., 2015, pp. 448–456.
- [55] A. F. Agarap, "Deep learning using rectified linear units (ReLU)," *CoRR*, vol. abs/1803.08375, 2018.
- [56] D. P. Kingma and J. Ba, "Adam: A method for stochastic optimization," in *Proceedings of the International Conference on Learning Representations (ICLR)*, 2015.